Both predictability and familiarity facilitate contour integration

Michaël Sassi Laboratory of Experimental Psychology, University of Leuven, Leuven, Belgium

Maarten Demeyer Laboratory of Experimental Psychology, University of Leuven, Leuven, Belgium

Bart Machilsen Laboratory of Experimental Psychology, University of Leuven, Leuven, Belgium

Tom Putzeys Laboratory of Experimental Psychology, University of Leuven, Leuven, Belgium

Johan Wagemans Laboratory of Experimental Psychology, University of Leuven, Leuven, Belgium

Research has shown that contour detection is impaired in the visual periphery for snake-shaped Gabor contours but not for circular and elliptical contours. This discrepancy in findings could be due to differences in intrinsic shape properties, including shape closure and curvature variation, as well as to differences in stimulus predictability and familiarity. In a detection task using only circular contours, the target shape is both more familiar and more predictable to the observer compared with a detection task in which a different snake-shaped contour is presented on each trial. In this study, we investigated the effects of stimulus familiarity and predictability on contour integration by manipulating and disentangling the familiarity and predictability of snake-like stimuli. We manipulated stimulus familiarity by extensively training observers with one particular snake shape. Predictability was varied by alternating trial blocks with only a single target shape and trial blocks with multiple target shapes. Our results show that both predictability and familiarity facilitated contour integration, which constitutes novel behavioral evidence for the adaptivity of the contour integration mechanism in humans. If familiarity or predictability facilitated contour integration in the periphery specifically, this could explain the discrepant findings obtained with snake contours as compared with circles or ellipses. However, we found that their facilitatory effects did not differ between central and peripheral vision and thus cannot explain that particular discrepancy in the literature.

Introduction

Human vision depends crucially on grouping together those parts of the retinal image that belong to the same object. Traditionally, much research in this domain has been focused on contour integration (Loffler, 2008; Wagemans et al., 2012a), the process by which local line or edge elements are linked together into more complex object contours. The now standard contour integration paradigm and the related notion of a local association field (AF) were introduced by Field, Hayes, and Hess (1993). The typical stimulus contains a contour path consisting of several Gabor elements, embedded in additional distracter Gabors. Field et al. (1993) used open-ended, snake-like contour shapes and found that such contours are readily detected as long as the path elements are given positions and orientations consistent with a smooth underlying contour, which essentially demonstrates the Gestalt principle of good continuation (Hess, May, & Dumoulin, in press; Wagemans et al., 2012a).

Performance in contour integration tasks varies as a function of the relative positions and orientations of neighboring elements along the contour path. The angle formed by each pair of consecutive elements is one important parameter: Detectability decreases gradually as the path angle increases, although detection performance in the study by Field et al.

Citation: Sassi, M., Demeyer, M., Machilsen, B., Putzeys, T., & Wagemans, J. (2014). Both predictability and familiarity facilitate contour integration. *Journal of Vision, 14*(5):11, 1–15, http://www.journalofvision.org/content/14/5/11, doi:10.1167/14.5.11.

doi: 10.1167/14.5.11 Received December 20, 2013; published May 30, 2014 ISSN 1534-7362

(1993) remained significantly above chance level up to interelement angles of 60°. The same authors also found that contour linking is strongest when the constituent Gabor elements have perfectly curvilinear orientations (i.e., are each oriented along a tangent of the underlying contour). Performance deteriorated gradually with the addition of jitter to the path elements' orientations. These basic findings of increased detectability or discriminability of straight versus more curved contour paths (e.g., Hess, Beaudot, & Mullen, 2001; Sassi, Machilsen, & Wagemans, 2012) and of the importance of curvilinear orientations along the path (e.g., Bex, Simmers, & Dakin, 2001; Dakin & Baruch, 2009; Sassi et al., 2012) have been replicated numerous times (see Hess et al., in press, for a recent review).

In sum, the literature suggests that performance in contour integration tasks depends primarily on the local good continuation between neighboring elements. Likewise, the underlying linking mechanism is generally hypothesized to rely on lateral interactions between cells in the primary visual cortex (V1). Roughly speaking, models such as Field et al.'s (1993) AF explain contour integration in terms of local interactions between the neurons responding to a given contour element and those responding to neighboring contour elements. Integration takes place for certain spatial interrelations between elements—corresponding to the AF, namely collinearity and cocircularity—but not for others. Elements with suitable interrelations become linked into a continuous chain of activation, which causes the smooth contour as a whole to pop out from the background. The AF model was originally conceived on the basis of psychophysical findings, but there is indeed physiological evidence for anisotropy in the horizontal connections within V1. Excitatory connections between neurons with nearby but non-overlapping receptive fields are found mostly between neurons tuned to collinear and cocircular orientations (see Loffler, 2008, for a review), providing a plausible neural basis for the Gestalt principle of good continuation. The AF remains a key concept in more advanced contour integration models such as that of Ernst et al. (2012; see also Van Humbeeck, Schmitt, Hermens, Wagemans, & Ernst, 2013), who used several AF-like sets of linking probabilities to generate different "ensembles" of stimuli and then characterized a single general-purpose AF that predicted human performance across all of their stimuli.

Although the local alignment of collinear or cocircular elements is crucial to contour integration, it has been shown that larger-scale contour properties, such as the global object shape, contribute as well. Here, we focus especially on a study by Kuai and Yu (2006), who investigated contour integration in peripheral vision using circular and elliptical contours. Earlier studies of contour integration in peripheral vision had shown clearly impaired performance compared with central vision (Hess & Dakin, 1999; Nugent, Keswani, Woods, & Peli, 2003) for open-ended snake contours that differed in shape between trials, like those used by Field et al. (1993). Kuai and Yu (2006) used only circular and elliptical contours centered on fixation and manipulated eccentricity by increasing or decreasing the contour radius. With this method, performance remained unaffected up to 35° eccentricity in detection tasks and up to 20° in discrimination tasks. Kuai and Yu (2006, p. 1412) attributed this "constant peripheral contour integration" to the "good Gestalt nature" of the circular and elliptical contours, which of course raises the question of what determines their Gestaltness.

Several possible explanations for the "good Gestalt nature" of Kuai and Yu's (2006) contours relate primarily to their intrinsic simplicity—that is, the regularities present in the contour shapes. As the authors themselves noted, the snake contours used in earlier studies (Hess & Dakin, 1999; Nugent et al., 2003) are open-ended and change direction randomly from element to element, whereas the circles and ellipses in their study are closed shapes whose contours have a constant direction of curvature. Both unidirectionality of curvature (Pettet, 1999; Pettet, McKee, & Grzywacz, 1998) and closure (Braun, 1999; Kovacs & Julesz, 1993; Mathes & Fahle, 2007; but see Tversky, Geisler, & Perry, 2004, for an important caveat) can facilitate contour integration. Two additional factors not explicitly mentioned by Kuai and Yu (2006) are that the circles and ellipses in their experiments, unlike snake contours, were entirely convex with respect to fixation and were mirror symmetric. Contour integration in the periphery has been shown to be faster for convex than for concave contours (Machilsen, Demeyer, & Wagemans, 2013), and mirror symmetry may provide a slight integration benefit for closed contours centered on fixation (Machilsen, Pauwels, & Wagemans, 2009), although this has not been tested with contour radii or eccentricities comparable with those of Kuai and Yu (2006).

For the present study, however, we focused on factors related to the observer's expectations and past experience rather than intrinsic properties of the contour shapes. We identified two such factors and investigated (a) whether they facilitate contour integration in general and (b) whether they enhance the robustness of contour integration in the visual periphery specifically (as described by Kuai & Yu, 2006).

First, Kuai and Yu (2006, p. 1418) already pointed out that "knowing at least roughly what the to-be-detected contour looks like" may have played a role in preserving the integration of circular and elliptical contours in the periphery. Their observers knew to

expect circular or elliptical shapes rather than a new randomly generated snake on every trial. Physiological studies have shown that attention and expectation modulate V1 activity during contour integration (Ito & Gilbert, 1999; Li, Piëch, & Gilbert, 2004, 2006). In a recent study, McManus, Li, and Gilbert (2011) recorded single cells in macaque V1 while the monkeys performed a delayed-match-to-sample contour integration task. They found that the tuning of single neurons in macaque V1 changed depending on the cued shape and showed that the AF is adaptive and that subsets of lateral interactions can be inhibited or activated depending on the task. Following that rationale, a human observer in a contour integration experiment who knows the global shape of the target contour beforehand will be tuned to that particular shape. That shape may then acquire "good Gestalt" properties in the sense that its integration is facilitated over that of other shapes. We henceforth refer to this factor as the predictability of the target shape.

A second factor, which Kuai and Yu (2006) did not consider, is that circles and ellipses not only occur predictably in their experiment but are also familiar shapes to any human observer. Familiarity has been shown to influence figure-ground assignment (see Peterson, in press, for a comprehensive review), but its effect on contour integration has not been directly tested. The familiarity of shapes often entails that they have a certain meaning to the observer and are immediately recognized and apprehended (as, e.g., a circle or an ellipse), but essentially familiar shapes are simply shapes with which the observer has much past experience. This past experience might in itself explain the preferential or "good Gestalt" status of such shapes. For the present study, we therefore operationally define shape familiarity as the quality of having occurred with high frequency within the context of the experiment. Thus defined, the familiarity of shapes can be experimentally manipulated.

In what follows, we report an experiment in which we manipulated and disentangled shape predictability and familiarity and tested their effects on performance in a two-interval forced choice (2IFC) contour detection task. The primary aim of the current study was to test whether predictability or familiarity, or both, facilitate peripheral contour integration. In light of the findings of Kuai and Yu (2006), we additionally investigated whether these effects are specific to peripheral vision or whether they could, *given an equal level of perceptual uncertainty*, apply equally to central vision. We used a set of inherently unfamiliar snake-like contours (comparable with those of Field et al., 1993; Hess & Dakin, 1999; Nugent et al., 2003), all generated by the same algorithm to control for intrinsic simplicity-related shape properties as described above.

The experiment consisted of two phases. In the training phase, observers extensively practiced 2IFC detection of one particular snake shape. We used a different shape for each observer, effectively manipulating shape familiarity between subjects. During the subsequent test phase we alternated two types of trial blocks: blocks where the target was the trained shape on every trial, and mixed-shape blocks where the target differed between trials. In test blocks containing only the trained shape, the target shape was thus both familiar and predictable. In test blocks containing the mixed-shape blocks, 10% of trials contained the trained, familiar shape as the target. On these trials, the target shape was thus familiar but unpredictable. The remaining mixed-shape block trials consisted of a mix of nine untrained snake shapes that differed from block to block and occurred on 10% of trials each. Hence, within the mixed-shape blocks, the occurrence of each unfamiliar shape was as equally unpredictable as that of the familiar shape.

This design allowed us to disentangle effects of predictability (differences in detectability of the familiar shape between trained-shape and mixed-shape blocks) and familiarity (differences in detectability of the familiar and unfamiliar shapes within mixed-shape blocks) and to conclude whether either of these factors can enhance the integration of particular snake contours compared with other contours of comparable complexity. Furthermore, by training and testing in both central and peripheral vision, we were able to test whether predictability or familiarity provided a contour integration benefit specific to the periphery, such as that observed by Kuai and Yu (2006).

Methods

Participants

Seven observers—four women and three men—between 20 and 27 years of age ($M = 23.4$, $SD = 2.7$) took part in the experiment. One was an expert observer from the lab who was aware of the aims of the study (observer KV); the remaining six were students taking part in exchange for either course credit or a small financial compensation and were not aware of the purpose of the experiment. KV knew that the familiar shape would appear occasionally during the mixed-shape blocks but never consciously recognized it (see Procedure), and omitting her data from the analysis did not change our conclusions with regard to the effects of predictability and familiarity (see Data analysis).

Total experiment duration ranged from 10 to 12 hr depending on the participant. The expert observer completed the experiment in two sessions on consecu-

tive days. The student participants completed the experiment in 3 to 4 consecutive days. All experiments complied with the tenets of the Declaration of Helsinki and the guidelines of the Ethics Committee of the Faculty of Psychology and Educational Sciences of the University of Leuven.

Apparatus

Participants viewed the stimuli from a distance of 57 cm on a gamma-corrected 20-in. Iiyama Vision Master Pro 514 CRT monitor (Iiyama International, Hoofddorp, The Netherlands) running at a resolution of 800 × 600 pixels and a refresh rate of 100 Hz. Eye movements were sampled at 1000 Hz by an SR Research EyeLink 1000 camera (SR Research Ltd., Mississauga, Canada) located in a desktop mount placed below the monitor at a camera-to-eye distance of approximately 50 cm. We programmed the experiment in Matlab, using Psychophysics Toolbox version 3 (Brainard, 1997; Kleiner, Brainard, & Pelli, 2007; Pelli, 1997) to control stimulus presentation and to interface with the EyeLink and the Palamedes toolbox (Kingdom & Prins, 2010; Prins & Kingdom, 2009) for the adaptive staircase procedures. We performed data analyses using SAS version 9.3 (SAS Institute Inc., Cary, NC) and PyMC version 2.3 (Patil, Huard, & Fonnesbeck, 2010) for Python.

Stimuli

Contour shapes

In conventional snake contours (e.g., Field et al., 1993; Hess & Dakin, 1999; Nugent et al., 2003) the underlying shape is a skeleton of straight contour segments rather than a smooth contour. The orientation of each segment differs from the previous one by a value known as the path angle. The sign of the path angle can change at random between segments and its magnitude is usually jittered by a small amount. Gabor elements are then placed at the center of each segment and, when aligned with the global orientation of the segment, the resulting Gabor display suggests a smooth contour.

Our experiment required repeated presentations of each shape, some of them thousands of times. We created more smoothly curved shapes so that we could repeatedly present the same global contour shape without repeating the exact same local element positions. Each segment of our contours consisted of 90 subsegments, each of which differed in orientation from the previous one by 1/90 of the path angle, so that the first and last subsegment of each segment differed in orientation by the path angle (plus the randomized path angle jitter; see below). The resulting contours allowed placement of tangentially oriented Gabors anywhere along the contour path.

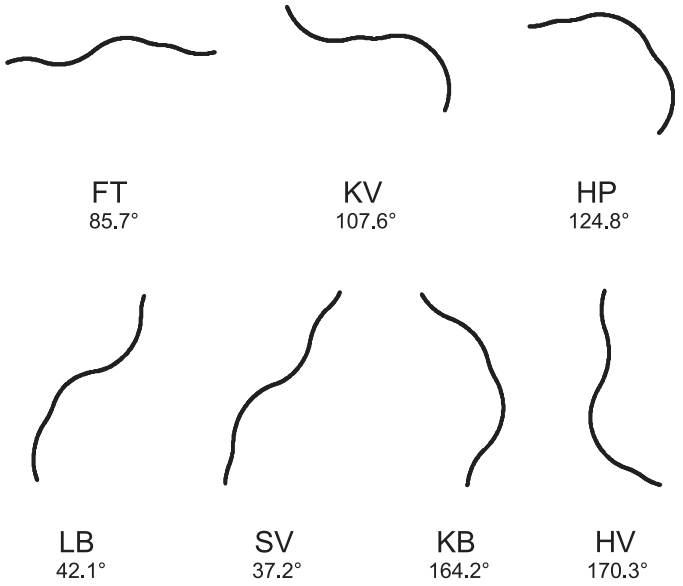

Figure 1. Examples of the contour shapes used in our experiment. Below each contour are the initials of the observer for whom that particular contour was the to-be-familiarized training shape (see also Figure 3) and the main axis orientation of the contour. Shapes are sorted by increasing deviation from horizontal (90°). These training shapes were selected by splitting the full set of 181 contour shapes into seven bins based on how much their main axis orientation differed from horizontal and then drawing one contour at random from each bin.

We created 181 such contours, each consisting of 12 segments (1,080 subsegments), with a path angle of 20° (plus a jitter drawn for each segment from a uniform distribution between −4° and 4°). In order to control complexity and to avoid contours with unidirectional curvature and contours with many direction changes that are approximately straight, we constrained the amount of direction changes between segments to be between three and five, situated at locations randomly selected from the 11 possible in between the 12 segments. Seven examples of the resulting contours are shown in Figure 1, which contains the to-be-familiarized training contour for each of the seven participants.

Gabor displays

All stimuli used throughout the experiment consisted of a contour embedded in a full-screen Gabor display of 40° × 30° of visual angle. Contours were exactly 264 pixels in length, which equaled 13 cm on our setup (see Apparatus). For trials with central presentation, we placed the contour's midpoint at a random location inside a 2° × 2° square area in the center of the screen.

For peripheral presentation we similarly jittered the global position within a 2° × 2° area centered 10° to the left or right of center. We then used the Grouping Elements Rendering Toolbox (GERT; Demeyer & Machilsen, 2012) for Matlab to place 12 odd-symmetric Gabor elements at equidistant locations along the contour—starting at a random location on the first segment and placing one element per segment—and fill the remainder of the array with randomly positioned distracter elements while controlling for local density using the Voronoi method available in the GERT. This method consists of performing a Voronoi tesselation to construct a polygon around each element, such that all coordinates within the polygon are closer to that element than to any other element in the display. Each element's local density metric is then computed as the surface area of this polygon, and a statistical test is performed to ascertain that there is no significant difference in the local density metric between elements along the contour and elements in the remainder of the array.

For every 2IFC trial in the experiment, we generated two new displays containing that trial's target contour. For each display separately, we repeated the process of jittering the global position of the contour, placing 12 equidistant contour elements starting from a random position on the first segment and filling the background with randomly positioned elements as described above. For the display used in the target-absent interval, we assigned random orientations to the contour elements to eliminate the good continuation cue defining the contour. In addition, the fact that a contour was also latently present in the distracter displays eliminated the effect of any potentially remaining density cue based on the element positions alone. Figure 2 shows an example of a target-present Gabor display with tangentially oriented contour elements and a target-absent display with randomized contour element orientations.

Training contour selection

Due to the horizontal and radial biases in contour integration (Schipper, Fahle, Stecher, & Ernst, 2011) and the fact that in the peripheral conditions the more horizontally oriented contours would extend to a point closer to fixation than more vertically oriented contours, the global orientation of the to-be-familiarized contour was a potential confounding factor. In order to sample the entire range of orientations, we first divided the 181 contours into seven equal-width bins depending on the absolute deviation of the contour's main axis orientation (obtained via singular value decomposition of the coordinate matrix of the contour's subsegments in Matlab) from horizontal (values ranging between 0° and 90°). One contour was then randomly selected from each bin and assigned as a training contour to one of the seven participants.

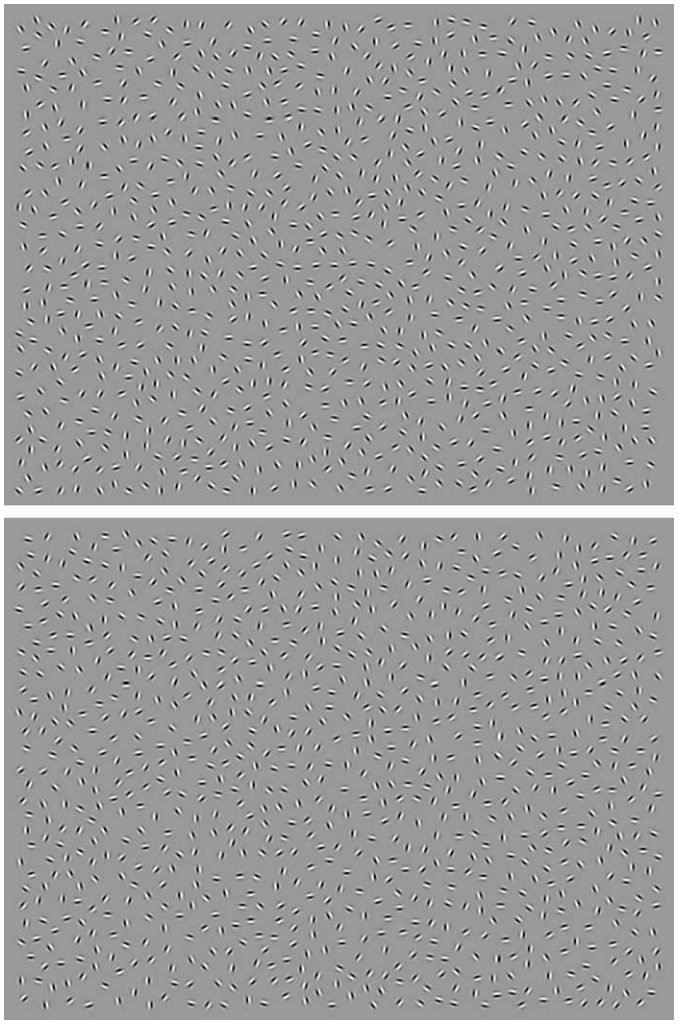

Figure 2. Full-screen target-present (top) and target-absent (bottom) Gabor displays used in the experiment. Both displays contain 12 Gabor elements placed along the training contour for observer KV (see Figure 1). These contour elements' orientations are tangential to the underlying contour in the target-present display (top) and randomized in the target-absent display (bottom).

Procedure

Task

The basic task throughout the experiment was 2IFC contour detection, performed in blocks of 100 trials each. Trials started with the presentation of a white fixation dot on a middle-gray background. Participants fixated the center of the screen and manually started each trial by pressing the space bar on the computer keyboard. Drift correction was then performed, after which the fixation dot remained onscreen for 100 ms, followed by two Gabor displays shown for 150 ms each, separated by a 300-ms blank middle-gray interstimulus interval. After the offset of the second stimulus interval, with the screen once again blanked to middle gray,

participants pressed the left or right arrow key to indicate whether the contour was perceived in the first or second interval, respectively. Fixation was monitored from drift correction until the end of the second stimulus interval, and trials were aborted whenever participants failed to maintain fixation within a 6° × 6° square area centered on the screen throughout this period.

Training phase

Each participant completed 24 training blocks of 100 trials in which the target was consistently their to-be-familiarized shape, with a different arrangement of Gabor elements on each trial (see Stimuli). Participants were explicitly told that the target was the same shape on every trial and they were allowed to view the smooth target shape between blocks (see Figure 1) if they wished to, but all participants quickly began to find this unnecessary as training progressed. The target position was either central or at 10° of eccentricity, alternating between blocks. Only one eccentric position was used throughout all phases of the experiment: either 10° to the left of fixation or 10° to the right, alternating between participants.

During the first four blocks, the orientations of the contour elements in the target-present interval were perfectly tangential to the underlying contour. During the remaining 20 blocks, orientation jitter was added to the contour elements in the target-present interval using an adaptive staircase procedure aiming at a performance of 81.65% correct. Each individual contour element's orientation jitter was drawn from a uniform distribution between plus and minus the current jitter value determined by the adaptive procedure. Each 100-trial block consisted of two randomly interleaved 50-trial one-up/two-down staircases with a $\Delta+$ (size of a step up) of 4° and a $\Delta-$ (size of a step down) of 2° of jitter. In other words, after every incorrect response the jitter level for that staircase decreased by 4° (increasing the intensity of the signal), and after two consecutive correct responses to trials of the same staircase 2° were added to the maximum jitter level (decreasing the intensity of the signal). Only responses from completed trials were taken into account. Trials aborted due to eye movements had no effect on the staircase.

At the end of every block the mean jitter level at all reversals except the first two in that block was calculated for each staircase separately, and these values served as the starting jitter levels for the two staircases in the next block with the same eccentricity. We targeted the same performance in the center and the periphery to avoid ceiling effects and to obtain a clear baseline of performance where the target is both predictable and familiar. This would allow us to conclude decisively whether any effects of predictability or familiarity were main effects across both eccentricities or interaction effects, differing in magnitude between central and peripheral vision. At the end of the 24-block training phase, we took the grand means of the mean jitter levels at all but the first two reversals for the last three central blocks and for the last three peripheral blocks and used the resulting jitter levels for the center and the periphery throughout the rest of the experiment.

The reader would be correct in concluding that the current study therefore does not (explicitly) test for the eccentricity effect itself in perceptual grouping, which was a main focus of Kuai and Yu's study. Since different jitter levels were used for central and eccentric stimuli, the absence of a main effect of eccentricity is expected—and in fact aimed at—since without equal baseline difficulty levels in eccentric and peripheral vision we could quickly run into floor or ceiling effects when studying their interaction with predictability or familiarity.

Test phase

During the test phase we alternated between blocks containing only the trained shape and blocks with many different target shapes. Regardless of block type, each individual contour element's orientation jitter in the target-present interval was drawn from a uniform distribution between plus and minus the reference jitter level obtained from the training phase.

In the trained-shape-only blocks, the shape that was familiarized during the training phase was presented on each trial. Participants were explicitly informed about this before the start of the block. In these blocks, the target shapes were both familiar and predictable.

The mixed-shape blocks contained several target shapes. On 10 out of 100 trials the target was the familiar shape, whereas the remaining 90 trials contained 10 instances of nine untrained shapes from the set of 181, so that within a given mixed-shape block the occurrence of each unfamiliar shape was as equally unpredictable as that of the familiar shape. The untrained shapes differed between blocks so that participants saw each untrained shape only 10 times during the entire experiment. Participants were not told that these blocks contained the familiar shape or that any of the shapes in these blocks were presented repeatedly. They were simply instructed that the targets would be different shapes of roughly similar length and complexity as the trained shape. These mixed-shape blocks trials where the target was the familiar shape thus provided data for the condition where the shape was unpredictable but familiar. Trials with untrained shapes constituted the condition where the target shape was both unpredictable and unfamiliar.

We alternated trained-shape-only blocks and mixed-shape blocks and central and peripheral (in the trained position, either 10° to the left or 10° to the right of

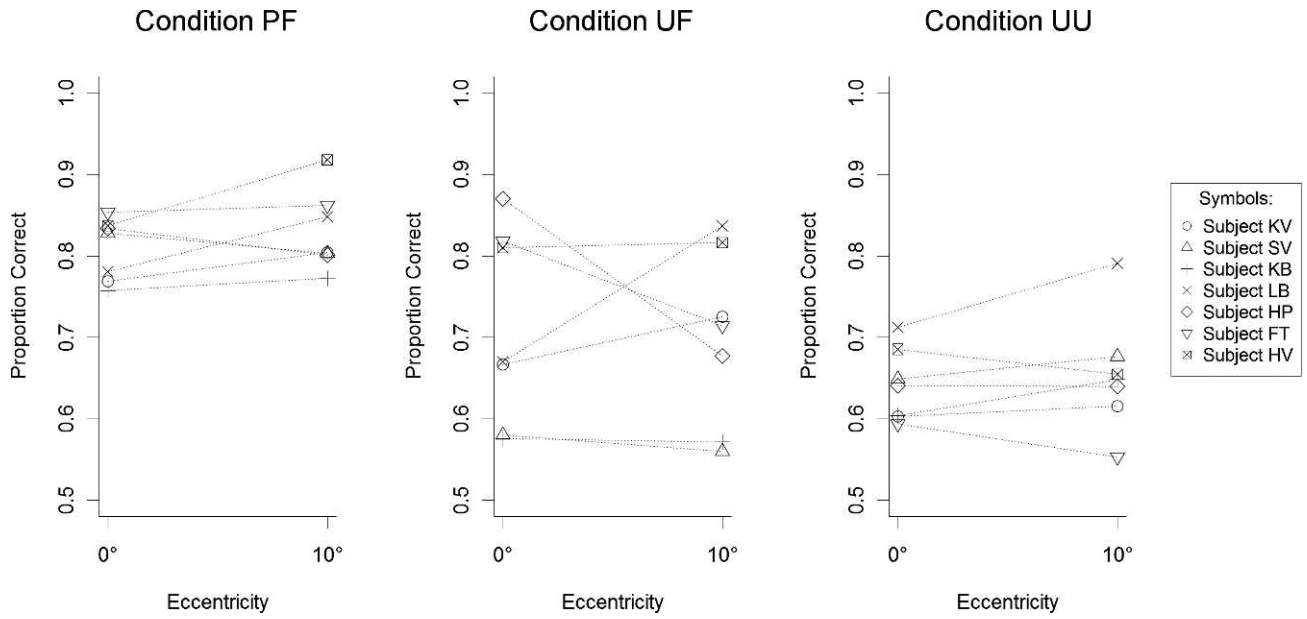

Figure 3. Proportions of correct contour detections for each individual observer by eccentricity (central or peripheral) and by predictability and familiarity condition: predictable and familiar (PF), unpredictable and familiar (UF), and unpredictable and unfamiliar (UU).

fixation, depending on the participant) presentation and repeated the resulting sequence of four block types (trained-shape-only central, mixed-shape central, trained-shape-only peripheral, mixed-shape peripheral) 10 times for a total of 40 blocks. We asked the student participants, after the experiment and before fully debriefing them, whether they had noticed anything about the shapes in the mixed-shape blocks and prompted further with the more specific questions of whether they had noticed repetitions of any shape and whether they had noticed that the familiar shape was included. Only one out of the six student participants had recognized the familiar contour on a small number of occasions, and none were aware that it or any other contour shape was being systematically repeated 10 times in the mixed-shape blocks. Even observer KV, who was aware that the familiar shape would occasionally appear during mixed-shape blocks, reported not consciously recognizing the trained contour shape in any test phase trial.

Results

Summary statistics

We analyzed the responses from all completed test phase trials. Maintaining central fixation proved to be fairly straightforward; aborted trials were rare even in blocks where the target was presented in peripheral vision. Depending on the observer, 38 to 120 test phase trials out of the total of 4,000 were aborted. Before exploring the data further, we checked our data for interval biases (Yeshurun, Carrasco, & Maloney, 2008). Comparing the interval biases for each observer in each of the four test block types, we found no evidence of any systematic biases either within or across observers or block types. We therefore carried out all further analyses under the assumption that sensitivity was overall equal in both intervals of the 2IFC task.

Figures 3 and 4 summarize the proportion correct per eccentricity and per condition within (Figure 3) and across (Figure 4) observers. Performance in trained-shape-only blocks, where the target shape was both predictable and familiar (PF), was as expected. The adaptive training procedure did not perfectly match difficulty between the center and the periphery in each individual observer, but averaged across observers, performance in the PF condition was close to the target of 81.65% in both the center (80.85%) and the periphery (83.02%).

Average performance in the untrained-shape trials in mixed blocks, where the target shape was unpredictable and unfamiliar (UU), was lower than that in the PF condition for all observers. Averaged across observers, performance was similarly impaired in the center (64.11%) and the periphery (65.42%) compared with the PF condition.

The data from trained-shape trials in mixed blocks, where the target shape was unpredictable but familiar (UF), were much noisier, as can be seen from the individual observers' means in Figure 3. This was a natural consequence of our design, which dictated that

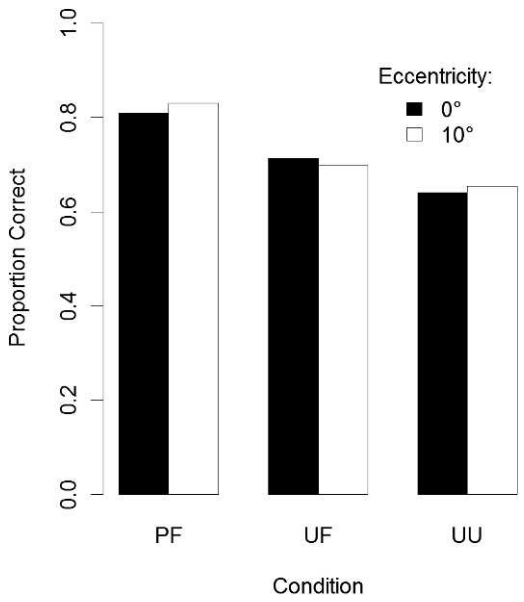

Figure 4. Proportions of correct contour detections by eccentricity (central or peripheral) and condition across all observers. The pooled data show a clear trend whereby performance was highest when the target shape was both predictable and familiar (PF), lower when the target shape was unpredictable but familiar (UF), and lower still when the target shape was both unpredictable and unfamiliar (UU).

there were very few observations in the UF condition (200 trials per observer, 100 per eccentricity, minus any aborted trials) compared with the PF (2,000 trials per observer, minus aborted trials) or UU (1,800 trials per observer, minus aborted trials) conditions. Five out of seven individual observers tended toward better performance in the UF condition than in the UU condition in either central or peripheral vision or both, whereas the remaining two showed no such effect and even tended toward the opposite effect. Averaged across observers a clearer trend emerged, showing better performance in the UF condition than in the UU condition (Figure 4). Within the UF condition, performance was again comparable in the center (71.31%) and the periphery (69.96%).

In sum, the trends in the data suggest that stimulus predictability and stimulus familiarity each facilitated contour integration and that their effects did not differ greatly between central and peripheral vision. The primary focus of our remaining analyses was to test the significance of these predictability and familiarity effects. Despite the large amount of data collected, analyses concerning the familiarity and predictability effects in particular had low statistical power at the individual level due to the nature of our design. We therefore carried out our analyses at the group level, taking care to encompass the considerable variability between observers in our statistical models.

Data analysis

Before fitting models to our data to further investigate the effects of predictability, familiarity, and eccentricity, we explored whether any covariates would make useful additions to the model. Although all 181 contour shapes used in this study were generated by the same algorithm and thus were exactly equal in length and approximately equal in terms of magnitude of curvature, we investigated three possible intrinsically shape-related confounds.

Given the potential importance of unidirectionality of curvature (Pettet, 1999; Pettet et al., 1998; see Introduction), we explored whether the amount of direction changes (three to five in our stimuli) had an effect. Additionally, since we reasoned that contours with long monotonically curved parts might have yielded an integration advantage regardless of the number of times the contour as a whole changed direction, we checked for any correlation between the length of the longest monotone segment in a contour and that contour's detection rate. We found no evidence for any systematic effect of either of these variables on performance and did not include them in our further analyses.

The third potential confound was a horizontal bias, due to the general horizontal and radial biases in contour integration (Schipper et al., 2011) or to the fact that in the peripheral conditions the more horizontally oriented contours would extend to a point closer to fixation than would more vertically oriented contours. There was indeed a global trend toward better performance for contours with near-horizontal main axes, and we included the main axis orientation (see Stimuli) as a covariate in all subsequent analyses.

Additionally, and separately from the analyses of the full data reported below, we investigated whether any learning of the unfamiliar contours, each presented 10 times, took place during the test phase. To this end, we fitted modified logistic regression models—with the logit link altered to have a lower asymptote at 0.50 to reflect the proper guess rate for a 2IFC task—to the responses from the UU condition only. These models contained a single binary categorical predictor variable that simply indicated whether responses belonged to one of the first five or the last five presentations of a particular contour. This had no effect on performance regardless of whether we analyzed responses from central ($p = 0.124$) and peripheral ($p = 0.764$) trials separately or pooled responses across eccentricities ($p = 0.191$). There was a slight trend toward a learning effect in the central trials, but performance for UU contours was not significantly better in late than in early presentations of the same contour according to any of our analyses.

Parameter	Estimate	*SE*	*t*	*p*
Condition PF vs. UF	0.976	0.234	4.18	0.001**
Condition UU vs. UF	−0.529	0.241	−2.19	0.049*
Eccentricity	0.198	0.106	1.86	0.112
Main axis[1]	−0.059	0.111	−0.54	0.611
Main axis[2]	−3.171	1.166	−2.72	0.030*

Table 1. Parameter estimates, standard errors, test statistic values, and *p*-values for the fixed effects in the final mixed logistic regression model. Superscripts denote the first and second order terms of the quadratic effect of main axis orientation. *Notes*: * $p < 0.05$; ** $p < 0.01$.

Generalized linear mixed model

We first fitted a mixed logistic regression model to our data, with the logit link modified to have a lower asymptote at 0.50 to reflect the actual guess rate in our 2IFC task. Mixed logistic regression models, also termed mixed logit models, combine ordinary logistic regression with random effects (Baayen, Davidson, & Bates, 2008; Bolker et al., 2009; Jaeger, 2008; Quené & Van Den Bergh, 2008). This allows analysis of the binary response variable at the group level while taking into account the clustering of observations by subject and the potential variability in effects between subjects.

We fitted the models using the SAS GLIMMIX procedure, starting from a model containing only fixed effects. Effects of predictability and familiarity entered the model as a condition factor with three levels: predictable and familiar (PF), unpredictable and familiar (UF), and unpredictable and unfamiliar (UU). Eccentricity was included as a factor with two levels (0° or 10°), and main axis orientation entered this analysis as a continuous variable ranging from 0° to 180°, with 90° being the horizontal orientation. We included a quadratic term in order to accurately model the curvilinear relationship of main axis to performance, whereby performance was enhanced for main axis orientations around 90° and lowered toward both near-vertical extremes of 0° and 180°. We found no significant interactions of the condition factor or main axis orientation with the eccentricity factor and therefore proceeded with the model containing fixed main effects of condition (familiarity and predictability), eccentricity, and main axis, all of which were significant at this point.

We then added covariance parameters (i.e., random effects), one at a time, to account for the between-subject variance of the intercept, the condition effects, the eccentricity effect, and the main axis orientation effect. We relied on the Bayesian information criterion (BIC) to decide on the inclusion of random effects. Since each addition resulted in a lowering of the BIC, all of the random effects parameters remained in the model. Ideally, we would then have readded the interactions and retested whether incorporating their intersubject variability through including random interaction effects could have lifted any of them to statistical significance. Unfortunately, however, the fitting procedure no longer converged on reliable estimates when we included the additional parameters, which precluded the fitting of more complex models.

Table 1 summarizes the output for the fixed effects parameters in the model. The main effect of eccentricity was no longer significant at $\alpha = 0.05$ in the final model ($p = 0.112$, but this parameter was nevertheless included since the corresponding random effect improved the model fit). The quadratic term of the main effect of main axis orientation proved significant ($p = 0.030$), confirming the horizontal bias. Predictability had a significant facilitatory effect on performance (condition PF vs. UF, $p = 0.001$). The evidence for a facilitatory effect of familiarity was inconclusive. The *p*-value for the UF versus UU comparison was strictly speaking just below the 0.05 criterion ($p = 0.049$). It could be argued, however, that this comparison should be Bonferroni corrected and that the *p*-value should have been below 0.025 in order for the effect to be considered significant since we tested two comparisons for the condition factor (PF vs. UF and UF vs. UU).

Bayesian data analysis

We were not entirely satisfied with the modified mixed logit model for two main reasons. First, as described above, once we had added the random effects parameters, we had apparently reached the limit of model complexity and could no longer include and test for interactions of predictability, familiarity, or main axis orientation with the eccentricity factor. Second, we believe that the inconclusive results with regard to the familiarity effect might also have been due to the inherent limitations of the mixed logit model.

Bayesian data analysis is well documented—although it is not yet in widespread use in cognitive science—and it is inherently more flexible in terms of model specification than are null hypothesis significance testing methods (Kruschke, 2010). In addition, the output of a Bayesian data analysis (the probability of an above-zero valued true condition parameter, given the data) provides a more intuitive answer to the question actually asked by a researcher than does a classical analysis (the probability of a sample at least as

extreme as the observed data, given a zero valued true condition parameter).

Bayesian modeling does allow us to fit a model including interactions of the main effects while simultaneously modeling the between-subject variability. An additional key difference is that the mixed logit model described in the previous section needs to encompass between-subject variability with regard to the main effects in one single variance component or parameter per main effect (see, e.g., Baayen et al., 2008). In our data, all subjects showed a clear predictability effect but the between-subject variability in the familiarity effect was considerable (see Figure 3). The Bayesian model allowed us to add a third hierarchical level, where besides the main effects parameters and their variances between subjects we additionally estimated the individual subjects' deviations from the group-level estimates of the main effects parameters.

We fitted a Bayesian model containing eight fixed effects parameters: an intercept parameter corresponding to baseline performance in the PF condition; main effects of eccentricity, predictability, familiarity, and main axis orientation (recoded here as absolute value deviations from 90°); and predictability × eccentricity, familiarity × eccentricity, and main axis × eccentricity interactions. For each of these fixed effects we also included a variance parameter, corresponding to the variance component representing the random effects in the mixed logit model, and individual random effect parameters (seven per main effect; i.e., one for each subject), constituting the additional third hierarchical level (compared with the mixed logit model) discussed in the previous paragraph.

The Bayesian model starts from a linked collection of parameters and prior beliefs about their values, which are specified in a prior distribution for each parameter. The model fitting procedure (see Appendix for details) then estimates the posterior probability distribution of the model. Rather than point estimates, this produces a posterior distribution for each parameter that directly reflects the probability of all possible parameter values given the data. These posterior distributions can then be used to test any hypothesis regarding the parameter values, including a null hypothesis where the parameter value equals zero, by computing whether the value of interest lies within the 95% highest density interval (HDI) of the parameter's posterior distribution.

Table 2 contains the medians, 95% HDIs, and proportion p of samples at least as extreme as zero (i.e., parameter values of zero or of opposite sign to the median) for each of the posterior distributions of the fixed main effects in our fitted model. The median value of the posterior distribution could be considered as resembling a point estimate for the parameter. Note that due to the nature of Bayesian modeling, the proportions p here can be directly interpreted as reflecting the probability that the true parameter value is zero or of opposite sign to the median given the data (unlike a traditional null hypothesis test, which evaluates the likelihood of samples at least as extreme as the observed data given the null hypothesis; see also Kruschke, 2010).

Parameter	Median	95% HDI	p
Predictability	−0.76	[1.19; 0.34]	0.004**
Familiarity	−0.66	[1.10; 0.24]	0.001**
Eccentricity	0.48	[0.20; 0.84]	0.001**
Predictability × eccentricity	0.36	[0.82; 0.08]	0.110
Familiarity × eccentricity	0.31	[0.21; 0.87]	0.247
Main axis	−0.91	[1.57; 0.35]	0.009**
Main axis × eccentricity	−0.52	[1.18; 0.01]	0.056

Table 2. Median, 95% highest density interval (HDI), and proportion p of samples more extreme than zero for each of the posterior probability distributions of the fixed effects in the Bayesian statistical model. *Notes*: ** $p < 0.01$.

Applying a 0.05 criterion for the proportion of samples at least as extreme as the zero value for each posterior distribution, none of the interaction terms in the model proved significant, but the Bayesian model found strong evidence for all of the main effects. The facilitatory effects of both predictability (proportion $p = 0.004$) and familiarity (proportion $p = 0.001$) were clearly significant, as was the main axis effect reflecting a horizontal bias (proportion $p = 0.009$). There was a significant main effect of eccentricity, whereby performance was significantly better in the periphery than in central vision (proportion $p < 0.001$). Finally, since observer KV was aware of the aims of the study, we refitted the same model using only the data of the six naïve observers. This analysis is not reported here in detail as its conclusions for the most part matched those obtained when analyzing the full data set and confirmed the presence of main effects of both predictability and familiarity. The only difference was in the significance of the main axis × eccentricity interaction (proportion p using the data of the six naïve observers = 0.036; proportion p using all data = 0.056).

Discussion

Our data showed evidence for facilitatory effects of two factors, which we termed predictability and familiarity, on performance in a contour detection task. Within the context of our experiment, predictability refers to knowing what the to-be-detected contour on the current trial will look like, and familiarity refers to having seen that target shape many times before. Our

paradigm was specifically designed to disentangle these two factors, to test their effects in both central and peripheral vision, and to control for potential confounding variables. We used snake-like contours (e.g., Field et al., 1993; Hess & Dakin, 1999; Nugent et al., 2003) that were all of comparable complexity and not inherently familiar, and we manipulated familiarity by means of extensive training with a different contour for each observer.

We tested the significance of the facilitatory effects of both predictability and familiarity by fitting two statistical models to our data. The first was a generalized linear mixed model, namely a modified mixed logistic model (Baayen et al., 2008), which showed clear evidence for an effect of predictability but arguably inconclusive evidence for the familiarity effect. We analyzed the data a second time using a Bayesian model, which to date is less commonly used for data analysis in cognitive science (Kruschke, 2010) but which we consider to be more appropriate for the current data. Compared with the generalized linear mixed model, the Bayesian model found more conclusive evidence for a facilitatory effect of familiarity.

In sum, we identified the predictability and familiarity of the contour shape as two independently contributing factors underlying more robust contour integration of snake-like contours. These findings provide novel behavioral evidence for a top-down controlled, adaptive contour integration mechanism in humans, analogous to the adaptivity shown in macaque V1 by McManus et al. (2011). The facilitatory effect of predictability illustrates how the contour integration mechanism can consciously be tuned to particular expected signals. The familiarity effect suggests that adaptivity also goes beyond this conscious anticipation of specific stimuli: There seems to be an unconscious learning of, or adaptation to, the statistics of the current visual environment.

If familiarity or predictability facilitate contour integration in the periphery specifically, then this could explain the difference in the findings obtained with circles or ellipses (Kuai & Yu, 2006) as compared with snake contours (Hess & Dakin, 1999; Nugent et al., 2003). The effects we found, however, were main effects across both eccentricities. Performance for unpredictable or unfamiliar contours was not more affected in the periphery than in central vision, and predictability and familiarity therefore cannot explain the remarkable preservation of contour integration in the periphery reported by Kuai and Yu (2006). It remains an open question what exactly constitutes the "good Gestalt nature" of the circular and elliptical contours they used, by which they explain their results.

The central unifying principle in classical early 20th-century Gestalt theory is the law of Prägnanz or "goodness," from which the more specific grouping principles such as good continuation, closure, symmetry, parallelism, and so on are derived (Pomerantz & Kubovy, 1986; Wagemans, Wichmann, & Op de Beeck, 2005). The law of Prägnanz is often equated to the simplicity principle, which holds that what we perceive is the "simplest" possible organization of the proximal stimulus or, in other words, the organization that best captures the regularities in the input (van der Helm, in press; Wagemans et al., 2012b). The Gestalt school considered the processes that capture these regularities to be autonomous and intrinsic to the observer, and consequently the presence or absence in the stimulus of the regularities to which these processes are sensitive determines the "goodness" of the organized percept.

The focus on intrinsic simplicity in the Gestalt school of thought is in contrast with the Helmholtzian view, in which likelihood is the central principle. According to the likelihood principle, the proximal stimulus is interpreted in terms of what its most likely distal source is, via an unconscious inference process (Pomerantz & Kubovy, 1986; Wagemans et al., 2005, 2012b). Because determining which organization is more likely implies knowledge of the probability of occurrence of objects or events, this view places greater emphasis on the role of past experiences and learning. It follows from the likelihood principle that a particular organization could be preferred, or in Gestalt terms "better," because we know it—consciously or unconsciously—to be a likely occurrence.

The effects of predictability and familiarity found in the present study constitute evidence for the core tenet of the likelihood school: that frequencies and probabilities of occurrence affect perceptual organization. However, our results do not detract from the importance of shape properties that are traditionally regarded as related to intrinsic simplicity. The two principles are far from being mutually exclusive and, in fact, the distinction between them has been called into question. Simplicity-based explanations fit a likelihood-based framework equally well if one assumes that simpler interpretations also correspond to more likely occurrences, and there have been attempts along these lines to reconcile the two principles, with some authors arguing that the two are ultimately equivalent (Chater, 1996; Feldman, 2009; van der Helm, 2000; see Wagemans et al., 2012b, for an in-depth discussion).

We deliberately did not focus our study on the effects of intrinsic shape properties such as closure, convexity, or symmetry—by controlling for them rather than manipulating them—but these properties have previously been shown to influence contour integration (Machilsen et al., 2009, 2013; Mathes & Fahle, 2007). Consequently, the particular "goodness" of a Gestalt of Kuai and Yu's (2006) circular and elliptical contours that caused integration benefits specific to the periphery may indeed involve the

intrinsic regularity of the target shapes. Our results neither corroborate nor contradict such an explanation. In any case, the present study did isolate two novel nonlocal factors influencing contour integration, and the remaining discrepancy between our findings and those of Kuai and Yu (2006) suggests that more such factors underlying the "goodness" of a Gestalt remain to be identified. This shows that contour integration is not governed solely by the local interactions included in typical AF models and raises the question of how these nonlocal factors influence the integration mechanism. Evidence from single cell recordings in macaque V1 (McManus et al., 2011) suggests that this is accomplished by adaptive, top-down controlled tuning of the local AF.

Besides the predictability and familiarity effects that were of main interest here, we found an effect of eccentricity, with significantly better performance in the periphery. First, this effect has no bearing on our conclusions with regard to the effects of predictability or familiarity as neither interacted with the eccentricity factor. Second, the presence of this effect does not mean that contour integration in the periphery was easier per se since we used an adaptive procedure during the training phase intended to equalize performance at both eccentricities to 81.65%. For all participants, this procedure applied more jitter in central vision (39°–49°) than in the periphery (12°–39°) to arrive at the targeted performance. This places our results in line with earlier findings of impaired contour integration in the periphery for snake contours (Hess & Dakin, 1999; Nugent et al., 2003). Although the adaptive procedure approximately achieved the desired result, the Bayesian analysis suggests that it may for some reason still have systematically slightly underestimated the tolerance to orientation jitter in the periphery, resulting in a small performance difference between the center and the periphery that carried over to the test phase (see Figures 3 and 4).

Finally, there was a significant effect of main axis orientation of the contour shape, whereby detection was facilitated for near-horizontal orientations. This is in line with the findings of a general horizontal and radial bias in contour integration (Schipper et al., 2011). There was a trend for this effect to be more pronounced in the periphery, which may be related to the aforementioned radial bias or to the fact that the more horizontally oriented contours would extend to a point closer to fixation than would more vertically oriented contours when presented in the periphery. The Bayesian model indeed hinted at such an interaction (proportion $p = 0.056$; see Table 2), although it did not meet our 0.05 criterion in the analysis of the full data set. Incidentally, this interaction was significant when we performed an analysis without the data of observer KV (proportion $p = 0.036$).

Conclusions

In sum, we found evidence for facilitatory effects of predictability and familiarity on performance in a contour detection task, regardless of whether stimuli were presented in central or peripheral vision. Our findings add to the growing evidence of a role for top-down feedback in contour integration (Gilad, Meirovitzh, & Slovin, 2013; Ito & Gilbert, 1999; Li et al., 2004, 2006; Loffler, 2008). Specifically, the behavioral effect of predictability we demonstrate here in human observers mirrors the effects of expectation on the local AF found by McManus et al. (2011) in macaque V1. The presence of a familiarity effect in our data suggests that such adaptive tuning in V1 may not be restricted to those situations where a specific shape is anticipated and that there may well be a more general adaptation to the average statistics of the current visual environment, consistent with a likelihood approach to perceptual grouping (Wagemans et al., 2012b).

Keywords: contour integration, perceptual organization, shape perception, detection

Acknowledgments

This work was supported by a Methusalem grant from the Flemish Government (METH/08/02), awarded to Johan Wagemans, and by postdoctoral fellowships of the Fund for Scientific Research Flanders (FWO), awarded to Maarten Demeyer and Bart Machilsen.

Commercial relationships: none.
Corresponding author: Johan Wagemans.
Email: johan.wagemans@ppw.kuleuven.be.
Address: Laboratory of Experimental Psychology, University of Leuven, Leuven, Belgium.

References

Baayen, R. H., Davidson, D. J., & Bates, D. M. (2008). Mixed-effects modeling with crossed random effects for subjects and items. *Journal of Memory and Language, 59,* 390–412.

Bex, P. J., Simmers, A. J., & Dakin, C. (2001). Snakes and ladders: The role of temporal modulation in visual contour integration. *Vision Research, 41,* 3775–3782.

Bolker, B. M., Brooks, M. E., Clark, C. J., Geange, S. W., Poulsen, J. R., Stevens, M. H. H., & White,

J.-S. S. (2009). Generalized linear mixed models: A practical guide for ecology and evolution. *Trends in Ecology and Evolution, 24*(3), 127–135.

Brainard, D. H. (1997). The psychophysics toolbox. *Spatial Vision, 10,* 433–436.

Braun, J. (1999). On the detection of salient contours. *Spatial Vision*, *12*(2), 211–225.

Chater, N. (1996). Reconciling simplicity and likelihood principles in perceptual organization. *Psychological Review, 103,* 566–581.

Dakin, S. C., & Baruch, N. J. (2009). Context influences contour integration. *Journal of Vision*, *9*(2):13, 1–13, http://www.journalofvision.org/content/9/2/13, doi:10.1167/9.2.13. [PubMed] [Article]

Demeyer, M., & Machilsen, B. (2012). The construction of perceptual grouping displays using GERT. *Behavior Research Methods, 44,* 439–446.

Ernst, U. A., Mandon, S., Schinkel-Bielefeld, N., Neitzel, S., Kreiter, A. K., & Pawelzik, K. R. (2012). Optimality of human contour integration. *PLoS Computational Biology, 8*(5), e1002520, 1–17, doi:10.1371/journal.pcbi.1002520.

Feldman, J. (2009). Bayes and the simplicity principle in perception. *Psychological Review, 116,* 875–887.

Field, D. J., Hayes, A., & Hess, R. F. (1993). Contour integration by the human visual system: Evidence for a local "association field." *Vision Research, 33,* 173–193.

Gilad, A., Meirovitzh, E., & Slovin, H. (2013). Population responses to contour integration: Early encoding of discrete elements and late perceptual grouping. *Neuron*, *78*(2), 389–402.

Hess, R. F., Beaudot, W. H. A., & Mullen, K. T. (2001). Dynamics of contour integration. *Vision Research, 41,* 1023–1037.

Hess, R. F., & Dakin, S. C. (1999). Contour integration in the peripheral field. *Vision Research, 39,* 947–959.

Hess, R. F., May, K. A., & Dumoulin, S. O. (in press). Contour integration: Psychophysical, neurophysiological and computational perspectives. In J. Wagemans (Ed.), *Oxford handbook of perceptual organization*. Oxford: Oxford University Press.

Ito, M., & Gilbert, C. D. (1999). Attention modulates contextual influences in the primary visual cortex of alert monkeys. *Neuron, 22,* 593–604.

Jaeger, T. F. (2008). Categorical data analysis: Away from ANOVAs (transformation or not) and towards logit mixed models. *Journal of Memory and Language, 59,* 434–446.

Kingdom, F. A. A., & Prins, N. (2010). *Psychophysics: A practical introduction*. London: Academic Press.

Kleiner, M., Brainard, D., & Pelli, D. (2007). What's new in Psychtoolbox-3? *Perception, 36*(ECVP Abstract Supplement), 14.

Kovacs, I., & Julesz, B. (1993). A closed curve is much more than an incomplete one: Effect of closure in figure ground segmentation. *Proceedings of the National Academy of Sciences, USA, 90*(16), 7495–7497.

Kruschke, J. K. (2010). What to believe: Bayesian methods for data analysis. *Trends in Cognitive Sciences*, *14*(7), 293–300.

Kuai, S., & Yu, C. (2006). Constant contour integration in peripheral vision for stimuli with good Gestalt properties. *Journal of Vision, 6*(12):7, 1412–1420, http://www.journalofvision.org/content/6/12/7/, doi:10.1167/6.12.7. [PubMed] [Article]

Li, W., Piëch, V., & Gilbert, C. D. (2006). Contour saliency in primary visual cortex. *Neuron, 50,* 951–962.

Li, W., Piëch, V., & Gilbert, C. D. (2004). Perceptual learning and top-down influences in primary visual cortex. *Nature Neuroscience, 7,* 651–657.

Loffler, G. (2008). Perception of contours and shapes: Low and intermediate stage mechanisms. *Vision Research, 48,* 2106–2127.

Machilsen, B., Demeyer, M., & Wagemans, J. (2013). Peripheral contour integration is biased towards convex contours. *Perception, 42*(ECVP Abstract Supplement), 115.

Machilsen, B., Pauwels, M., & Wagemans, J. (2009). The role of vertical mirror symmetry in visual shape detection. *Journal of Vision, 9*(12):11, 1–11, http://journalofvision.org/content/9/12/11/, doi:10.1167/9.12.11. [PubMed] [Article]

Mathes, B., & Fahle, M. (2007). Closure facilitates contour integration. *Vision Research, 47,* 818–827.

McManus, J. N. J., Li, W., & Gilbert, C. D. (2011). Adaptive shape processing in primary visual cortex. *Proceedings of the National Academy of Sciences, USA, 108*(24), 9739–9746.

Nugent, A. K., Keswani, R. N., Woods, R. L., & Peli, E. (2003). Contour integration in peripheral vision reduces gradually with eccentricity. *Vision Research, 43,* 2427–2437.

Patil, A., Huard, D., & Fonnesbeck, C. J. (2010). PyMC: Bayesian stochastic modelling in Python. *Journal of Statistical Software, 35*(4), 1–81.

Pelli, D. G. (1997). The VideoToolbox software for visual psychophysics: Transforming numbers into movies. *Spatial Vision, 10,* 437–442.

Peterson, M. A. (in press). Low-level and high-level contributions to figure-ground organization. In J. Wagemans (Ed.), *Oxford handbook of perceptual organization*. Oxford: Oxford University Press.

Pettet, M. W. (1999). Shape and contour detection. *Vision Research*, *39*(3), 551–557.

Pettet, M. W., McKee, S. P., & Grzywacz, N. M. (1998). Constraints on long range interactions mediating contour detection. *Vision Research*, *38*(6), 865–880.

Pomerantz, J. R., & Kubovy, M. (1986). Theoretical approaches to perceptual organization: Simplicity and likelihood principles. In K. R. Boff, L. Kaufman, & J. P. Thomas (Eds.), *Handbook of perception and human performance* (pp. 36-1–36-46). New York: Wiley.

Prins, N., & Kingdom, F. A. A. (2009). Palamedes: Matlab routines for analyzing psychophysical data. Retrieved from www.palamedestoolbox.org.

Quené, H., & Van Den Bergh, H. (2008). Examples of mixed-effects modeling with crossed random effects and with binomial data. *Journal of Memory and Language, 59,* 413–425.

Sassi, M., Machilsen, B., & Wagemans, J. (2012). Shape detection of Gaborized outline versions of everyday objects. *i-Perception, 3*(8), 745–764, doi: 10.1068/i0499.

Schipper, M., Fahle, M., Stecher, H., & Ernst, U. (2011). Human contour integration is independently biased by global stimulus shape and behavioural task: Evidence from psychophysics and electrophysiology. *Perception, 40*(ECVP Abstract Supplement), 210.

Tversky, T., Geisler, W. S., & Perry, J. S. (2004). Contour grouping: Closure effects are explained by good continuation and proximity. *Vision Research, 44,* 2769–2777.

van der Helm, P. A. (in press). Simplicity in perceptual organization. In J. Wagemans (Ed.), *Oxford handbook of perceptual organization*. Oxford: Oxford University Press.

van der Helm, P. A. (2000). Simplicity versus likelihood in visual perception: From surprisals to precisals. *Psychological Bulletin, 126,* 770–800.

Van Humbeeck, N., Schmitt, N., Hermens, F., Wagemans, J., & Ernst, U. (2013). The role of eye movements in a contour detection task. *Journal of Vision, 13*(14):5, 1–19, http://journalofvision.org/content/13/14/5/, doi:10.1167/13.14.5. [PubMed] [Article]

Wagemans, J., Elder, J. H., Kubovy, M., Palmer, S. E., Peterson, M. A., Singh, M., et al. (2012a). A century of Gestalt psychology in visual perception: I. Perceptual grouping and figure-ground organization. *Psychological Bulletin*, *138*(6), 1172–1217.

Wagemans, J., Feldman, J., Gepshtein, S., Kimchi, R., Pomerantz, J. R., van der Helm, P., et al. (2012b). A century of Gestalt psychology in visual perception: II. Conceptual and theoretical foundations. *Psychological Bulletin*, *138*(6), 1218–1252.

Wagemans, J., Wichmann, F. A., & Op de Beeck, H. (2005). Visual perception I: Basic principles. In K. Lamberts & R. Goldstone (Eds.), *Handbook of cognition* (pp. 3–47). London: Sage.

Yeshurun, Y., Carrasco, M., & Maloney, L. (2008). Bias and sensitivity in two-interval forced choice procedures: Tests of the difference model. *Vision Research, 48,* 1837–1851.

Appendix

We used a Markov Chain Monte Carlo (MCMC) procedure controlled by a Metropolis random walk (the default method in PyMC version 2.3; see Patil et al., 2010) to fit the Bayesian model. The model contained eight normally distributed fixed effects parameters. The intercept parameter corresponded to baseline performance in the PF condition and was given a strong prior ($SD = 0.5$ on the logit scale) since we knew the adaptive procedure had targeted 81.65% for this condition. The main effect of eccentricity was given the same strong prior since we knew the adaptive procedure targeted the same performance at both eccentricities in the reference PF condition. In the absence of strong prior knowledge, one specifies so-called weak or noninformative priors, which simply prevent the parameter from assuming impossible values. The remaining six fixed effects parameters in the model were given such weak priors ($SD = 10$ on the logit scale). These included effect parameters for predictability, familiarity, main axis orientation (expressed as absolute deviations from 90°), and the predictability × eccentricity, familiarity × eccentricity, and main axis × eccentricity interactions.

For each of the eight fixed effects we also included a variance parameter corresponding to the variance component representing the random effects in the mixed logit model. The variance parameters were given gamma prior distributions to avoid negative values. Following the rationale from the fixed effects, the variance parameters for the intercept and the eccentricity main effect were given stronger priors (scale = 1, rate = 0.01) than were the remaining six variance parameters (scale = 1.5, rate = 0.01). Finally, we added the individual random effect parameters (seven per

main effect; i.e., one for each subject) and specified their distributions as normal with the applicable fixed main effect parameter as the mean and the applicable variance parameter as the variance. In Bayesian logic, this pushes the assumption of normally distributed random effects, present in both the logit mixed model and the current model, to its full consequence; namely, that the raw subject variance isn't automatically also the variance of the normally distributed random effects term but that the real subject variance itself is a parameter to be estimated, given the observed individual data and given the assumption of a normal distribution.

The modified logistic link function with a lower asymptote at 0.50 was included as a so-called deterministic node, whose single value per trial is entirely determined by the combination of the other parameters, and the data as the observed node (Patil et al., 2010). All parameters in the model were sampled using PyMC's default Metropolis step method. We repeated the MCMC sampling procedure 12 times. For each of the 12 chains we discarded the first 20,000 samples as burn-in and kept every 100th sample out of the remaining 50,000 to avoid autocorrelated samples, yielding 500 samples per chain (see Patil et al., 2010, for an explanation of burn-in and sample thinning). We pooled the samples from all chains and then determined the medians, 95% HDIs, and proportion p of samples at least as extreme as zero (i.e., parameter values of zero or of opposite sign to the median) for each of the posterior distributions of the fixed main effects, as reported in Table 2.